General self-imaging properties in $N \times N$ multimode interference couplers including phase relations

M. Bachmann, P. A. Besse, and H. Melchior

Self-imaging properties of generalized $N \times N$ multimode interference couplers are derived. Positions, amplitudes, and phases of the self-images are directly related to the lengths and widths of the coupler by solving the eigenmode superposition equation analytically for any arbitrary length. Devices of length $(M/N)\,3L_c$, where M is the multiple occurrence of the N self-images, are analyzed in detail. The general formalism is applied to practical $N \times N$ couplers used in integrated optics, and simple phase relations are obtained.

Key words: Integrated optics, optical splitters and combiners, self-imaging.

1. Introduction

Splitting and combining of multiple optical beams is an important function in integrated optics. Multimode waveguides can be used to form multiple images. Ulrich and Ankele,[1] after a suggestion by Bryngdahl,[2] first demonstrated this effect in planar glass waveguides. Using ray optics, they successfully described the formation of multiple images at certain device lengths. The phases of the images, however, have not been given in a compact analytic expression. Ten years later, Niemeier and Ulrich[3] reported a self-imaging 4×4 coupler in planar glass.

More recently, passive multimode interference (MMI) couplers with waveguides have been realized in different material systems. Self-imaging 2×2 devices that use Al_2O_3/SiO_2 waveguides,[4] InGaAsP/InP single heterostructures,[5] and InGaAsP/InP double heterostructures,[6] have been reported. Recently, 1×4 devices[7] and 4×4 couplers[8] have been fabricated. Beam splitters of the $1 \times N$ type, with N up to 20, have been demonstrated in the GaAs/AlGaAs material system.[9]

MMI couplers have promising characteristics. Accurate splitting ratios can be achieved. Most devices exhibit low excess losses of less than 0.5 dB in comparison with straight waveguides. Record low values for cross talk and imbalance have been reported. It has also been demonstrated that these values can be maintained fairly independently of polarization and over wide ranges of operation wavelengths[6] and operating temperatures.[5] Usually, 2×2 devices are short, well below 1 mm.[4–6] Even ultrashort (only 20–30-μm-long) 3-dB splitters have been reported.[10] Soldano *et al.* demonstrated good fabrication tolerances by optimizing the widths of the MMI couplers.[6]

Because of their superior performance, MMI couplers are beginning to be applied in more complex devices such as polarization-insensitive 2×2 Mach–Zehnder switches,[11,12] polarization-diversity photodetctors,[13] and optical hybrids for phase-diversity receivers.[8]

In addition to significant experimental progress, investigations of the theoretical aspects of MMI couplers have been published. Ulrich and Ankele[1] used ray optics to describe self-imaging phenomena. Another analysis by Chang and Kuester[14] used a decomposition into Green's functions. For $1 \times N$ splitters with a Dirac function $\delta(x)$ at the center of the MMI coupler as input excitation, the imaging formula has been given without derivation.[7] The phases of the images have not been derived explicitly for general $N \times N$ devices yet. They are, however, most important for designing more complex components based on optical interference, such as generalized $N \times N$ Mach–Zehnder switches, phase-diversity receivers, or devices for wavelength-division multiplexing. Taking the phases of the images into account, we

The authors are with the Institute of Quantum Electronics, Swiss Federal Institute of Technology, CH-8093 Zurich, Switzerland.

Received 1 June 1993; revised manuscript received 20 October 1993.

0003-6935/94/183905-07$06.00/0.

have already generalized the principle of Mach–Zehnder switches[15] with $N \times N$ MMI couplers as power splitters and combiners.

In this paper a theoretical derivation of the complete self-imaging properties, which leads to compact expressions for the positions, amplitudes, and phases of the images, is given for the first time, to our knowledge. We solve the eigenmode superposition equation analytically. Our theory describes any kind of MMI coupler. Specifically considered are MMI couplers of length $(M/N)\,3L_c$, where L_c is the coupling length of the two lowest-order modes and M and N are any positive integers without a common divisor that permit the description of any arbitrary device length. N turns out to be the number of images (inputs and outputs), whereas M is just a multiple occurrence of the N images at different device lengths. It can be chosen to be $M = 1$ for short devices.

Arbitrary input light distributions are decomposed into the guided modes of the MMI section, propagated down the length of the MMI coupler and superimposed at the output. The resulting equation for the image in the output plane of the MMI coupler is analytically transformed to describe the output field as a superposition of N images. Expressions in closed form are found for positions, amplitudes, and phases of the images. The general result is applied to practical $N \times N$ couplers used in integrated optics.

2. Problem Definition

MMI couplers are widely used in guided wave optics. Figure 1 shows a schematic view of a 2×2 coupler. Inputs and outputs of the multimode section are realized as integrated optical waveguides. In general, light from one input channel is distributed to one or more output channels. Although the access waveguides usually carry only one single, symmetrical mode, our theory is developed for arbitrary input light distributions.

In many applications, such as the generalized Mach–Zehnder switch,[15] not only the intensity distribution but also the phases at the output of the MMI coupler are relevant. We therefore develop a fully analytical theory based on the superposition of mode amplitudes and rewrite the equations to obtain the positions, amplitudes, and phases of the self-images. The practical three-dimensional problem shown in Fig. 1 is reduced to two dimensions, as shown in Fig. 2, with the effective index method. The operating

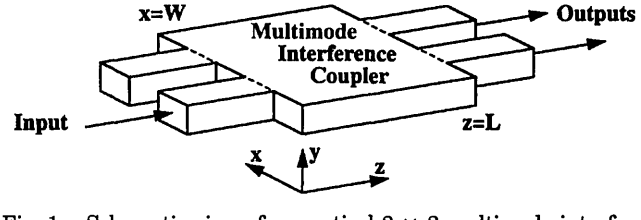

Fig. 1. Schematic view of a practical 2×2 multimode interference (MMI) coupler. Light from the input waveguide is launched into the MMI section, propagated, and imaged into the output waveguides.

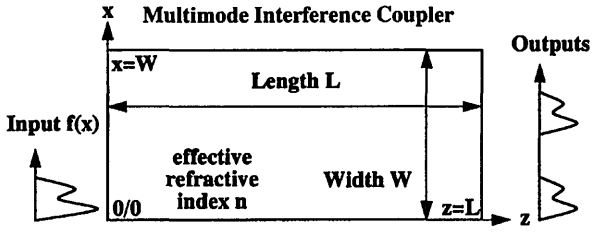

Fig. 2. General multimode interference coupler studied in this paper.

wavelength is λ. The MMI coupler has length L and width W, with the (effective) refractive index n (Fig. 2). The x and z axes that are chosen are defined in Figs. 1 and 2.

The theory developed in this paper describes the light propagation in the MMI section itself, including the generation of the images at certain lengths L of the MMI coupler. We do not include access waveguides at input and output to calculate losses, extinction ratios, or back reflections. However, we give the light distribution at any position within the MMI coupler in terms of images, which makes calculation of the above parameters easy.

3. Eigenmode Representation

A. Eigenmode Decomposition of the Input Field Distribution

The theory is developed for any input light distribution $f(x)$. This input distribution is decomposed into the eigenmodes of the MMI coupler. For complete decomposition, in general we need an infinite number of guided modes totally confined within the MMI section (strong guiding approximation). Resulting approximation errors have been investigated[16] and are negligible for strongly confined structures. For the practical case with a limited number of eigenmodes, the input distribution is decomposed into these eigenmodes, and the remaining field components are lost. This effect can be described with numerical mode analysis. The mode-decomposition theory, however, remains correct for practical applications, for which the input light distribution $f(x)$ is such that only guided modes and preferentially the lower-order modes are excited.

The optical-field distributions are shown in Fig. 3. For mathematical simplicity we added to the real MMI section a virtual section of equal width, as illustrated in Fig. 3, and extended eigenmodes and input distributions antisymmetrically to this virtual MMI section. The functions then are periodically extended to the whole x axis. This permits consideration of only the antisymmetrical functions with $2W$ periodicity. These functions can be Fourier decomposed with the eigenmodes. The $2W$ periodicity is useful in the derivation below.

The strongly guided eigenmodes of the MMI section have the form

$$E_i(x) = \sin\left[\pi(i+1)\frac{x}{W}\right] \qquad \text{with } i = 0, 1, 2, \ldots. \quad (1)$$

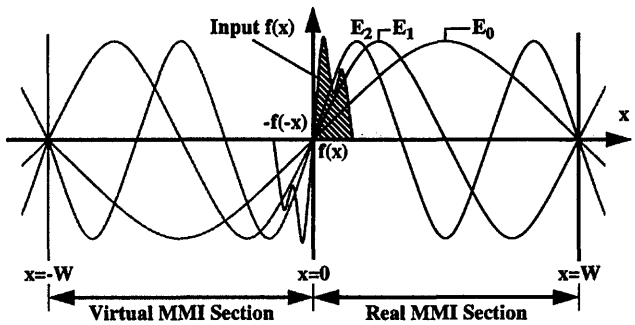

Fig. 3. MMI section with input light distribution $f(x)$ and decomposition into guided eigenmodes $E_i(x)$ of the structure. For theoretical purposes the functions $E_i(x)$ and $f(x)$ are antisymmetrically extended to a virtual MMI section and periodically repeated in the $\pm x$ directions.

Their propagation constants β_i are calculated in the paraxial approximation. Strongly guided modes are almost completely confined so that their lateral mode profiles will contain an integer number of half-periods within the waveguide. Therefore the transverse propagation constants are $k_{xi} = (i + 1)\pi/W$. The corresponding longitudinal propagation constants follow as $\beta_i^2 = n^2k_0^2 - k_{xi}^2$. Using paraxial approximation, we have $\beta_i \cong nk_0 - k_{xi}^2/2nk_0$, or with

$$\beta_0 \cong nk_0 - \frac{\Delta\beta_{01}}{3}, \qquad \Delta\beta_{01} = \beta_0 - \beta_1 \cong \frac{3\pi^2}{2nk_0W^2},$$

$$\beta_i \cong \beta_0 - i(i + 2)\frac{\Delta\beta_{01}}{3}, \tag{2}$$

where k_0 is the propagation constant in vacuum, $k_0 = 2\pi/\lambda$, and i is the mode number.

The incident light distribution $f(x)$ defined in the real MMI section $0 < x < W$ is extended to the virtual section $-W < x < 0$, forming the antisymmetrical function $g(x) = f(x) - f(-x)$. This function $g(x)$ is extended over the entire x axis with $2W$ periodicity and named $f_{in}(x)$ (Fig. 3). Using a spatial Fourier decomposition, we can rewrite $f_{in}(x)$ as a superposition of the infinite number of strongly guided eigenmodes $E_i(x)$ with the coefficients a_i:

$$f_{in}(x) = \sum_{i=0}^{\infty} a_iE_i(x), \qquad a_i = \frac{2}{W}\int_0^W f(x)E_i^*(x)dx. \tag{3}$$

Note that the functions $f(x)$ and $f_{in}(x)$ are identical in the actual MMI coupler between $0 < x < W$, where the real physical problem is defined.

B. Output Field Distribution

We investigate MMI couplers of fixed length L_N^M:

$$L_N^M = \frac{M}{N}3L_c = \frac{M}{N}\frac{3\pi}{\Delta\beta_{01}}, \tag{4}$$

where L_c is the coupling length between the two lowest-order modes $L_c = \pi/\Delta\beta_{01}$. M and N are any positive integers without a common divisor. This permits the analysis of any arbitrary device length. In addition, the two numbers have a physical meaning that will become clear at the end of the paper: N is the number of self-images, and M defines several possible device lengths with N images. Short devices are obtained for $M = 1$.

The input field is decomposed into the eigenmodes in Eq. (3) that propagate over the length L_N^M with the propagation constants β_i given in relations (2). At L_N^M they add up to the output field $f_{out}(x)$:

$$f_{out}(x) = \sum_{i=0}^{\infty} a_iE_i(x)\exp(-j\beta_iL_N^M). \tag{5}$$

Using relations (2) and Eq. (4), we can write this as

$$f_{out}(x) = \sum_{i=0}^{\infty} a_iA_iE_i(x),$$

$$A_i = \exp\left[-j\beta_0L_N^M + j\pi\frac{M}{N}i(i + 2)\right]. \tag{6}$$

The output of the MMI coupler is represented as a superposition of eigenmodes. The coefficients have a physical meaning: A_i accounts for the phase change of mode i. They can be calculated recursively, which is needed for the derivation of the self-imaging properties:

$$A_0 = \exp(-j\beta_0L_N^M), \quad A_i = A_{i-1}\exp\left[j\pi\frac{M}{N}(2i + 1)\right]. \tag{7}$$

4. From Eigenmodes to Self-Images

We have given the output light distribution $f_{out}(x)$ in the eigenmode superposition equation (6). The occurrence of multiple images is not obvious in this form. The positions, phases, and amplitudes of multiple images cannot easily be extracted from Eq. (6). We rewrite the output distribution so as to see the multiple images of the input $f_{in}(x)$ in the equations. Positions, amplitudes, and phases of the images will be obvious in such a representation.

A. Result: Output as Superposition of Images

First we give the equations obtained after rewriting Eq. (6). The different mathematical manipulations used are summarized afterward.

$$f_{out}(x) = \frac{1}{C}\sum_{q=0}^{N-1} f_{in}(x - x_q)\exp(j\varphi_q). \tag{8}$$

We have a sum of N images with equal amplitudes numbered by $q = 0, 1, \ldots, N - 1$. The positions x_q and phases φ_q of the images q are

$$x_q = (2q - N)\frac{M}{N}W, \tag{9}$$

$$\varphi_q = q(N - q)\frac{M}{N}\pi. \tag{10}$$

Note our definition of the phase $\varphi = \omega t - kz$. It increases at a fixed position z with increasing time t.

C is the complex normalization constant:

$$C = \exp(j\beta_0 L_N{}^M) \sum_{q=0}^{N-1} \exp\left[-j\pi \frac{x_q}{W} + j\varphi_q\right],$$

$$C = \exp\left(j\beta_0 L_N{}^M + j\pi \frac{M}{N}\right) \sum_{q=0}^{N-1} \exp\left[j\pi \frac{M}{N} q(N-q)\right]. \tag{11}$$

Because energy conservation is fulfilled, we have $|C| = \sqrt{N}$.

For $M = 1$, we use the reciprocity law for generalized Gaussian sums[17] and find that

$$C = \sqrt{N} \exp\left[j\beta_0 L_N{}^{M=1} + j\frac{\pi}{N} + j\frac{\pi}{4}(N-1)\right]. \tag{12}$$

Proofs of Eqs. (8)–(11) are outlined here and given in detail in Appendix A.

The coefficients A_i in the eigenmode superposition equation (6) are reformulated as follows: We introduce the coefficients B_i, which then are shown to be identical to A_i. The parameters B_i use the phases $\Phi_{i,q}$.

$$B_i = \frac{1}{C} \sum_{q=0}^{N-1} \exp(j\Phi_{i,q}) \qquad \text{with } \Phi_{i,q}$$

$$= -\pi(i+1)\frac{x_q}{W} + \varphi_q. \tag{13}$$

We obtain the identity for $i = 0$ by insertion: $A_0 = B_0$.

To show the identity $A_i = B_i$ recursively, we compare $\Phi_{i-1,q}$ and $\Phi_{i,q-1}$. Using Eq. (13) with Eqs. (9) and (10), we obtain

$$\Phi_{i,q-1} = \Phi_{i-1,q} + \pi \frac{M}{N}(2i+1). \tag{14}$$

This not very obvious idea is most important for the whole derivation in this paper. Insertion of Eq. (14) into Eq. (13) yields the identical recursive relation for the coefficients B_i, as has been obtained in Eq. (7) for the coefficients A_i. With $A_0 = B_0$ we therefore conclude that $A_i = B_i$. Using this new form for A_i we arrive at the desired superposition (8) of images with simple mathematics, as demonstrated in Appendix A.

B. Interpretation in Terms of Images

MMI devices of length $L_N{}^M$ produce N-fold images of the extended input function $f_{in}(x)$ at their outputs. These images correspond to $2N$ images of the real input function $f(x)$ in the range $-W < 0 < W$. Half of the images are inverted, and half of the images are upright. The images may even be cut into two parts. This can be avoided for practical applications. The real MMI section $0 < x < W$ includes N images of $f(x)$, again inverted or upright.

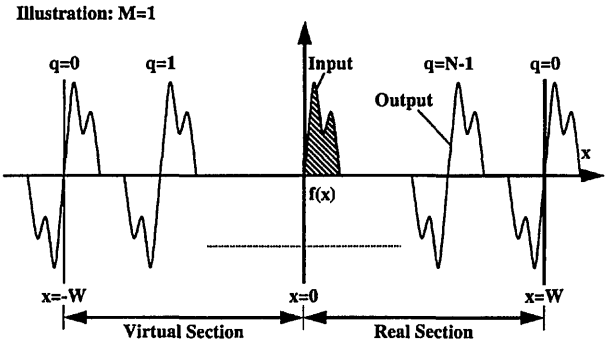

Fig. 4. MMI section with length $L_N{}^M$ produces N images of the extended input function $f_{in}(x)$. Here the case of $M = 1$ is illustrated. The real MMI section of width W contains N images of the real input $f(x)$ at the output. Images are partly inverted and partly upright. They may even be cut into two parts.

The case $M = 1$ is illustrated in Fig. 4. Of course the phases φ_q are not included in this simple drawing. The N-fold images of the extended input function $f_{in}(x)$ are numbered with q. Remember that the physical problem is defined in the real MMI section only. For the calculation of $f_{out}(x)$, terms with contributions to this limited range must be taken into account.

For general M the N-fold images are distributed over the range $-MW < x < MW$. Because all functions have $2W$ periodicity, each image has its correspondent in the range $-W < 0 < W$. Thus again we obtain $2N$ images of the real input function $f(x)$ in this range, a result simlar to the case of $M = 1$ in Fig. 4. Note that the numbering of these images is not straightforward anymore.

If N and M have a common divisor, two or more images are at the same place because of the $2W$ periodicity. This case has been excluded in our derivation without loss of generality.

5. Application to Practical $N \times N$ MMI Couplers with $M = 1$

A. Assumptions for Practical Devices

So far we have considered the case of arbitrary input light distributions. Practical applications of integrated optical MMI couplers, however, use waveguides as inputs and outputs. Waveguides restrict exciting and collecting light distributions to only limited ranges. For properly designed MMI couplers, different images of the input field at the output do not overlap. For this practical case, the results in Section 4 are simplified here for a better understanding and easier application.

For most practical applications, integrated optical devices should be as short as possible. In MMI couplers this is achieved with $M = 1$. We therefore consider a MMI coupler of length $L_N{}^{M=1} = 3L_c/N$, as given in Eq. (4). An access waveguide with spatially restricted input light distribution is placed at an arbitrary input position. N-fold images are formed at the output positions in Eq. (9). We obtain the other input positions with equal output image posi-

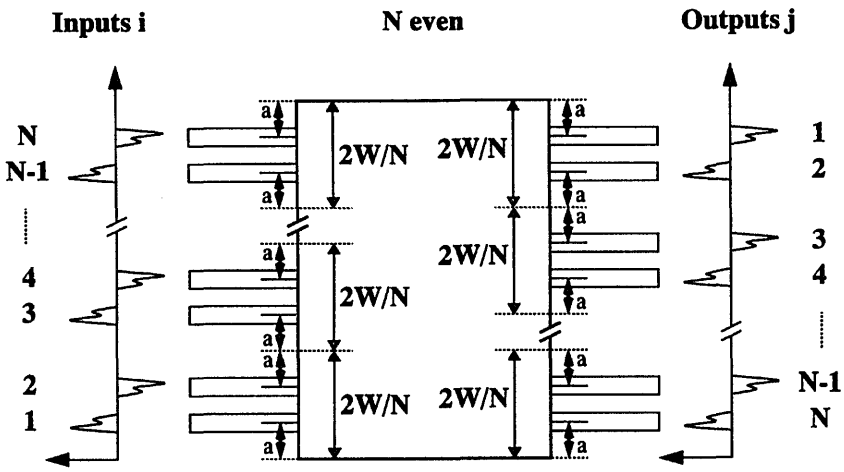

Fig. 5. MMI coupler with access waveguides illustrating the case of N even. Inputs are numbered bottom-up with index i and outputs are numbered top-down with j.

tions but different phases by using the MMI coupler in the backward direction. For properly positioned access waveguides, the self-images are smoothly coupled into the output waveguides, and reflections do not occur.

The situation is illustrated for N even in Fig. 5 and for N odd in Fig. 6. Note that the light distributions of the waveguides still do not have to be symmetrical, which permits, for example, the use of curved access waveguides. The derivation of the phases for general N is given below.

B. Derivation of the Phases for General N ($M = 1$)

The possible positions and the orientations of nonsymmetrical input and output distributions are found from Eqs. (8) and (9) and are illustrated in Fig. 4.

For a given width W and a chosen number of images N we obtain an additional free parameter a for the input and the output positions that is limited to $0 < a < W/N$. Figure 5 shows the situation for N even, and Fig. 6 shows the situation for N odd. Inputs are numbered with indices i, and outputs are numbered with indices j. Note the direction of the numbering: inputs bottom up and outputs top down.

The resulting phases for imaging input i to output j can be given now in a very compact form (remember our definition of the phase $\varphi = \omega t - kz$):

$$i + j \text{ even:} \quad \varphi_{ij} = \pi + \varphi_{N-(j-i)/2} = \varphi_o + \pi + \frac{\pi}{4N} \times (j - i)(2N - j + i),$$

$$i + j \text{ odd:} \quad \varphi_{ij} = \varphi_{N-(j+i-1)/2} = \varphi_o + \frac{\pi}{4N}(j + i - 1) \times (2N - j - i + 1), \tag{15}$$

where φ_o is the constant phase explicitly given by

$$\varphi_o = -\beta_0 L_N^{M=1} - \frac{\pi}{N} - \frac{\pi}{4}(N - 1). \tag{16}$$

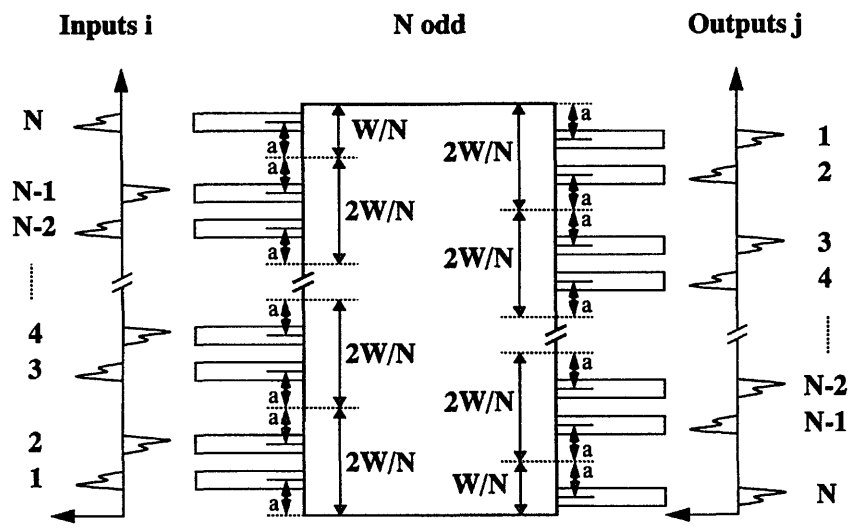

Fig. 6. MMI coupler with access waveguides illustrating the case of N odd.

Equations (15) and (16) are obtained as follows: To find the relative phases φ_{ij} for imaging input channel i to output channel j, we have to find the correct q values of Eq. (10). This is done by comparing Fig. 4 with Figs. 5 and 6. Care must be taken to include the minus sign or an additional phase π for inverted images, which occur for $i + j$ even. Note that q values outside of the range $0 \le q \le N - 1$ cause no problem because $\varphi_{q+N} = \varphi_q - 2q\pi$ [see Eq. (10)] yields the same phase for q and $q + N$.

To give an example we chose input $i = 1$. Output channels with j' odd correspond to $q = N - (j' - 1)/2$, and even outputs have $q = N - j'/2$.

Now we look at the general input channel i as shifted from input $i = 1$ by $i - 1$. The q values stay the same if the output j' are also shifted. The correct shift of the outputs for equal q is again $i - 1$. The shift is downward, corresponding to $j = j' + (i - 1)$ for odd j', and upward, corresponding to $j = j' - (i - 1)$ for even j'. Replacing j' with the correct j, we obtain for

$$j' \text{ odd or } i + j \text{ even:} \quad q = N - (j - i)/2,$$

$$j' \text{ even or } i + j \text{ odd:} \quad q = N - (j + i - 1)/2. \quad (17)$$

Equations (15) are now easily obtained with the above q values in Eq. (10) for the phases. Note the inclusion of the additional phase π for $i + j$ even.

We have recently used the resulting equations (15) for the design of a generalized Mach–Zehnder switch.[15] In these devices a phase-shifting section containing N phase modulators is placed between different MMI couplers used as passive splitters and combiners. The design of 1×4 switches has been completed for a promising InP/InGaAsP waveguide structure. Driving conditions of the switch have been analyzed and polarization independency has been predicted.[15] This example shows the importance of the phase relations presented. In this paper we added the complete derivation of the formulas. In Ref. 15 we also gave formulas for the general $1 \times N$ and $2 \times N$ couplers. These have been derived starting with Eqs. (15) above.

Conclusions

Self-imaging properties in generalized $N \times N$ MMI couplers have been analyzed. An arbitrary input distribution is decomposed into eigenmodes of the MMI section, propagated, and synthesized at the output. The output light distribution is analytically rearranged into equations showing the sum of images, including their positions, amplitudes, and phases. In particular the phases of the images, including their derivation, have been given for the first time. The general formalism has been applied to practical $N \times N$ MMI couplers with access waveguides. Simple phase relations have been obtained. They permit the straightforward application of MMI couplers to sophisticated integrated optic devices such as generalized Mach–Zehnder switches, phase-diversity receivers, and phased arrays for wavelength (de)multiplexing.

Appendix A: Proofs of Eqs. (8)–(11)

The proofs of Eqs. (8)–(11) have already been outlined. Here we give the details.

1. Reformulation of the Coefficients A_i

First we show the identity $A_i = B_i$ with A_i defined in Eqs. (7) and B_i defined in Eq. (13) in more detail.

Insertion of C [Eqs. (11)] shows the identity for $i = 0$: $A_0 = B_0$. To prove $A_i = B_i$ recursively we compare $\Phi_{i-1,q}$ and $\Phi_{i,q-1}$ as defined in Eq. (13) and obtain Eq. (14), which yields a relation between B_i and B_{i-1} as follows: The term with index q of the sum [Eq. (13)] is replaced by $q - 1$. The N periodicity of the summands is used.

We obtain

$$B_i = B_{i-1} \exp\left[j\pi \frac{M}{N}(2i + 1)\right]. \quad (A1)$$

The same relation has been obtained in Eqs. (7) for the coefficients A_i. With $A_0 = B_0$ we conclude that $A_i = B_i$ or

$$A_i = \frac{1}{C} \sum_{q=0}^{N-1} \exp\left[-j\pi(i + 1)\frac{x_q}{W} + j\varphi_q\right]. \quad (A2)$$

Now x_q can be replaced with $-x_q$. We replace the summation index q of the sum with $N - q$. x_q is replaced with $-x_q$, and $\varphi_q = \varphi_{N-q}$. Using the N periodicity, we obtain

$$A_i = \frac{1}{C} \sum_{q=0}^{N-1} \exp\left[j\pi(i + 1)\frac{x_q}{W} + j\varphi_q\right]. \quad (A3)$$

Equations (A2) and (A3) both yield expressions for A_i that differ only in the sign of the exponential terms. Below these expressions are replaced with sine terms.

2. Superimposed Images at the Output

The new forms of A_i are now inserted into Eq. (6), the eigenmode representation of the output of the MMI section. Here we examine the term $A_iE_i(x)$. The explicit form of the eigenmodes $E_i(x)$ of Eq. (1) is inserted into Eq. (6) and replaced with the exponential functions with the identity $\sin(x) = 1/2j[\exp(jx) - \exp(-jx)]$. We obtain

$$A_iE_i(x) = \frac{1}{2j}\left\{A_i \exp\left[j\pi(i + 1)\frac{x}{W}\right] - A_i \exp\left[-j\pi(i + 1)\frac{x}{W}\right]\right\}. \quad (A4)$$

The coefficients A_i are inserted with Eqs. (A2) and (A3) for the two exponential terms, respectively. This permits the introduction of the shifted eigen-

modes $E_i(x - x_q)$ and results in a compact form:

$$A_iE_i(x) = \frac{1}{C}\sum_{q=0}^{N-1}\frac{1}{2j}\left\{\exp\left[j\pi(i+1)\frac{x-x_q}{W}\right] - \exp\left[-j\pi(i+1)\frac{x-x_q}{W}\right]\right\}\exp(j\varphi_q),$$

$$A_iE_i(x) = \frac{1}{C}\sum_{q=0}^{N-1}E_i(x-x_q)\exp(j\varphi_q). \quad \text{(A5)}$$

This form of $A_iE_i(x)$ is now inserted into the output function $f_{out}(x)$ of Eq. (6). After interchanging the two sums and using the Fourier expansion of $f_{in}(x)$ in Eqs. (3), we finally arrive at Eq. (8)

$$f_{out}(x) = \frac{1}{C}\sum_{q=0}^{N-1}\left[\sum_{i=0}^{\infty}a_iE_i(x-x_q)\right]\exp(j\varphi_q),$$

$$f_{out}(x) = \frac{1}{C}\sum_{q=0}^{N-1}f_{in}(x-x_q)\exp(j\varphi_q). \quad \text{(A6)}$$

We thank M. K. Smit and L. B. Soldano of Delft University of Technology for helpful discussions on MMI couplers. This study was done as part of the RACE-ATMOS project of the European Community and was supported by the Swiss Office of Education and Science.

References

1. R. Ulrich and G. Ankele, "Self-imaging in homogeneous planar optical waveguides," Appl. Phys. Lett. **27,** 337–339 (1975).
2. O. Bryngdahl, "Image formation using self-imaging techniques," J. Opt. Soc. Am. **63,** 416–419 (1973).
3. Th. Niemeier and R. Ulrich, "Quadrature outputs from fiber interferometer with 4 × 4 coupler," Opt. Lett. **11,** 677–679 (1986).
4. L. B. Soldano, F. B. Veerman, M. K. Smit, B. H. Verbeek, A. H. Dubost, and E. C. M. Pennings, "Planar monomode optical couplers based on multimode interference effects," J. Lightwave Technol. **10,** 1843–1849 (1992).
5. E. C. M. Pennings, R. J. Deri, A. Scherer, R. Bhat, T. R. Hayes, N. C. Andreadakis, M. K. Smit, L. B. Soldano, and R. J. Hawkins, "Ultracompact, low-loss directional couplers on InP based on self-imaging by multimode interference," Appl. Phys. Lett. **59,** 1926–1928 (1991).
6. L. B. Soldano, M. Bachmann, P. A. Besse, M. K. Smit, and H. Melchior, "Large optical bandwidth of InGaAsP/InP multimode interference 3-dB couplers," presented at the Sixth European Conference on Integrated Optics, Neuchatel, Switzerland, 18–22 April 1993.
7. A. Ferraras, F. Rodríguez, E. Gómez-Salas, J. L. de Miguel, and F. Hernández-Gil, "Design and fabrication of a InP/InGaAsP multimode power splitter," in *Integrated Photonics Research,* Vol. 10 of 1993 OSA Technical Digest Series (Optical Society of America, Washington, D.C., 1993), pp. 151–154.
8. E. C. M. Pennings, R. J. Deri, R. Bhat, T. R. Hayes, and N. C. Andreadakis, "Ultra-compact integrated all-passive optical 90° hybrid using self-imaging," in *Proceedings of the 18th European Conference on Optical Communication* (VDE Verlag, Berlin, 1992), Vol. 1, pp. 461–464.
9. J. M. Heaton, R. M. Jenkins, D. R. Wight, J. T. Parker, J. C. H. Birbeck, and K. P. Hilton, "Novel 1-to-*N* way integrated optical beam splitters using symmetric mode mixing in GaAs/AlGaAs multimode waveguides," Appl. Phys. Lett. **61,** 1754–1756 (1992).
10. L. B. Soldano, M. Bouda, M. K. Smit, and B. H. Verbeek, "New small-size single-mode optical power splitter based on multimode interference," in *Proceedings of the 18th European Conference on Optical Communication* (VDE Verlag, Berlin, 1992), Vol. 1, pp. 465–468.
11. J. E. Zucker, K. L. Jones, T. H. Chiu, B. Tell, and K. Brown-Goebeler, "Strained quantum wells for polarization-independent electrooptic waveguide switches," J. Lightwave Technol. **10,** 1926–1930 (1992).
12. M. Bachmann, M. K. Smit, P. A. Besse, E. Gini, H. Melchior, and L. B. Soldano, "Polarization-insensitive low-voltage optical waveguide switch using InGaAsP/InP four-port Mach–Zehnder interferometer," in *Optical Fiber Communication Conference and International Conference on Integrated Optics and Optical Fiber Communication,* Vol. 4 of 1993 OSA Technical Digest Series (Optical Society of America, Washington, D.C., 1993), pp. 32–33.
13. R. J. Deri, E. C. M. Pennings, A. Scherer, A. S. Gozdz, C. Caneau, N. C. Andreadakis, V. Shah, L. Curtis, R. J. Hawkins, J. B. D. Soole, and J.-I. Song, "Ultra-compact, monolithic integration of balanced, polarization-diversity photodetectors," in *Proceedings of the 18th European Conference on Optical Communication* (VDE Verlag, Berlin, 1992), pp. 457–460.
14. D. C. Chang and E. F. Kuester, "A hybrid method for paraxial beam propagation in multimode optical waveguides," IEEE Trans. Microwave Theory Tech. **MTT-29,** 923–933 (1981).
15. P. A. Besse, M. Bachmann, and H. Melchior, "Phase relations in multi-mode interference couplers and their application to generalized integrated Mach–Zehnder optical switches," presented at the Sixth European Conference on Integrated Optics, Neuchatel, Switzerland, 18–22 April 1993.
16. R. Ulrich and T. Kamiya, "Resolution of self-image in planar optical waveguides," J. Opt. Soc. Am. **68,** 583–592 (1978).
17. K. Chandrasekharan, *Introduction to Analytic Number Theory* (Springer-Verlag, Berlin, 1968), pp. 34–44.